EXPERIMENTS AND UNSTEADY CFD-CALCULATIONS OF THERMAL MIXING IN A T-JUNCTION

Johan Westin([1]), Farid Alavyoon([2]), Lars Andersson([3]), Pascal Veber([3]), Mats Henriksson([1]) and Claes Andersson([4])

([1]) Vattenfall Utveckling AB, SE-81426 Älvkarleby, SWEDEN

([2]) Forsmarks Kraftgrupp AB, SE-74203 Östhammar, SWEDEN

([3]) Onsala Ingenjörsbyrå AB, Magasinsgatan 11b, SE-43437 Kungsbacka, SWEDEN

([4]) Ringhals AB, SE-43022 Väröbacka, SWEDEN

Abstract

Thermal mixing in a T-junction has been studied for validation of CFD-calculations. Experiments were carried out in a 2/3-scale model of a typical T-junction in a nuclear power plant, and temperature fluctuations were measured near the pipe walls by means of thermocouples. Three different flow ratios between the hot and cold water were considered. The computational results show that both steady and unsteady RANS fail to predict a realistic mixing between the fluids. The results were significantly better with scale-resolving methods such as LES and DES, showing fairly good predictions of the mean temperatures near the wall. The calculations did however predict larger fluctuations and different frequencies than observed in the model tests. Grid refinements showed that more small-scale fluctuations appeared in the calculated flow fields, although the predicted mean and temperature fluctuations near the walls were only moderately affected.

Introduction

Unsteady temperature fluctuations in pipe systems can lead to thermal fatigue in the pipe walls, and there are examples from nuclear power plants where thermal fatigue have been the cause for leaking pipes. A possibility to reduce the risk for such problems is to install static mixers to enhance the mixing process. Static mixers have e.g. been developed at Vattenfall Utveckling AB since the early 1980's, and are installed in nuclear power plants. However, such devices are expensive to install, so there are significant costs to be avoided if the risk for thermal fatigue can be accurately predicted with calculations. To perform such a structural analysis requires an accurate description of both amplitudes and frequencies of the thermal fluctuations near the pipe walls, and it is desirable to use CFD (Computational Fluid Mechanics) to obtain this information. However, the standard CFD-methods based on RANS (Reynolds Averaged Navier-Stokes equations) have difficulties to provide accurate results for this flow situation. Since thermal mixing is an important topic, which also constitutes a challenge for the CFD-methods available today, it has attracted considerable attention in recent years (see e.g. [1]-[3]).

The present paper describes some results from validation efforts on mixing in a T-junction that has been carried out in Sweden. The work was financed by the Swedish Nuclear Utility Analysis Group ("BG-gruppen"), which consists of representatives from the three Swedish utilities Forsmarks Kraftgrupp AB, Ringhals AB and OKG AB. The purpose of the group is to stimulate the development and validation of computational methods for nuclear power applications.

All calculations are based on model tests with a T-junction carried out at Vattenfall Utveckling [4]. The calculations focus on three different test cases and have been performed in three different groups: Vattenfall Utveckling AB [5][6], Forsmarks Kraftgrupp AB [7] and Onsala Ingenjörsbyrå AB [8][9]. The results obtained from steady and unsteady calculations based on Reynolds Averaged Navier-Stokes (RANS) equations showed very poor results and are only mentioned briefly. Instead, the main focus of the paper is on scale-resolving methods such as Large Eddy Simulations (LES) and Detached Eddy Simulations (DES).

The present paper is organized as follows. Firstly, a description of the experimental set-up and the measurement technique is given. The computational models are briefly described, followed by the results and corresponding comparisons with experiments. The results are reported separately for the three considered test cases. Finally, conclusions are given based on the results for all three test cases.

Model tests

The model tests were carried at the Älvkarleby Laboratory, Vattenfall Utveckling. The test rig was built in connection with the hydraulic machinery laboratory.

Experimental set-up

The model was designed to simulate a typical T-junction in a nuclear power plant, using a model scale of 1:1.5. The horizontal cold water main pipe had a diameter (D_2) of 190 mm in the model tests, and the water temperature (T_2) was approximately 25°C. The vertical hot water branch pipe was connected from below to the main pipe, and had a diameter (D_1) of 123 mm and a water temperature (T_1) of approximately 60°C. The pipes were made of acrylic glass (plexiglass) to allow optical access. The experimental set-up also included upstream bends in order to obtain realistic flow conditions, and an outline of the model geometry is shown in Figure 1. The origin of the Cartesian coordinate system

(x,y,z) is at the centre of the T-junction, and the corresponding velocity components are denoted (u,v,w).

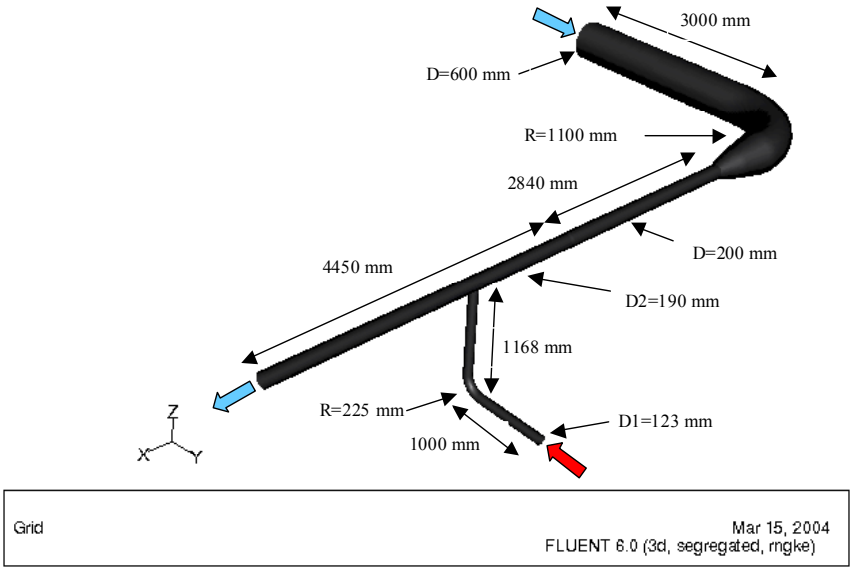

Figure 1 Model geometry (also used for simulations of test case 11).

The simulations of test case 11 were carried out on a model covering the geometry shown in Figure 1, while the simulations of test cases 9 and 10 used a smaller computational model shown in Figure 2.

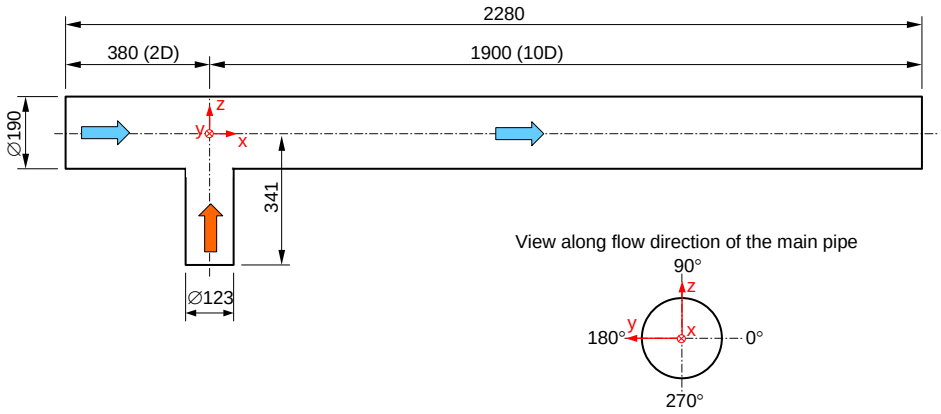

Figure 2 Smaller computational model used for test cases 9 and 10. See also definition of azimuth angles.

A hot water reservoir of 78 m^3 and a cold water reservoir of 300 m^3 were used, and the flow rates were measured with electromagnetic flow meters. Two Pt100-sensors measured the inlet temperatures of the hot and cold water. Moreover, approximately 35 thermocouples were used to measure the temperature fluctuations at a distance of 1 mm from the pipe walls at several positions downstream of the T-junction. The frequency response of the thermocouples were tested to be approximately 40-

50 Hz. All sensor signals were recorded with a data acquisition system at a sampling rate of 90 Hz, i.e. the maximum resolved frequency is 45 Hz in the measurements. The positions of the thermocouples are identified with the streamwise distance downstream of the T-junction, as well as an azimuth angle. The definition of the angles is shown in Figure 2

In addition to the temperature measurements flow visualizations were used. Also a limited number of velocity measurements were carried out using Pitot-tube and Laser Doppler Velocimetry (LDV). However, the quality of the velocity measurements was not sufficient, and the results are not shown in the present paper.

Test cases and presentation of data

A number of different ratios (Q_2/Q_1) between the cold (Q_2) and hot (Q_1) water flows were tested. Calculations have been carried out for three of the test cases, and the test conditions are summarized in Table 1. The penetration of the hot branch flow into the main pipe is significantly different between Test 9 and Test 11, which are illustrated in the flow visualizations in Figure 3. The mixing is characterized by large-scale fluctuations, which is more evident in the cases with smaller flow ratios (Test 10 and 11).

Table 1 Test conditions in the simulations.
(*) In the simulation of test 10 a constant viscosity was used which gave a slightly different Reynolds number in the hot water pipe.

Parameter	**Test 9**	**Test 10**	**Test 11**
Q_1 (l/s)	20	20	20
Q_2 (l/s)	112.5	56.3	47.8
Q_2/Q_1	**5.6**	**2.8**	**2.4**
T_1 (°C)	65.9	59.8	59.9
T_2 (°C)	27.3	24.0	25.7
Re_1	4.7×10^5	3.2×10^5 (*)	4.3×10^5
Re_2	8.8×10^5	5.8×10^5	3.6×10^5

To eliminate the effect of small temperature variations between different tests the measured data are normalized as follows:

$$T^* = \frac{T - T_{cold}}{T_{hot} - T_{cold}}$$

$$\frac{T_{rms}}{\Delta T} = \frac{T_{rms}}{T_{hot} - T_{cold}}$$

T_{rms}, T = mean and rms values of the temperature at the measurement position

T_{cold}, T_{hot} = cold and hot water temperatures at the main pipe and branch pipe inlets

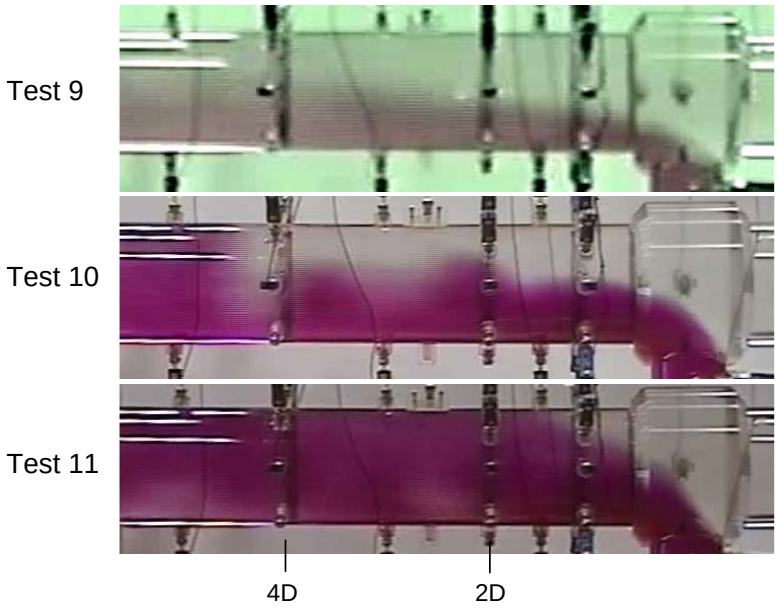

Figure 3 Flow visualizations for Test 9, 10 and 11. Flow direction is from right to left.

Computational models

Altogether several different models have been used in the present calculations, although the same models have not been used in all three calculations. Table 2 summarizes some of the numerical settings and material properties that were used in the LES- and DES-calculations.

Table 2 Numerical settings, material properties etc. for the LES- and DES-calculations.

Settings	**Test 9**	**Test 10**	**Test 11**
Fluent version	6.2.16	6.1.22	6.2.5
Model	DES and LES	LES	DES
DES-model	Spalart-Allmaras	-	Spalart-Allmaras
SGS-model (LES)	Dyn. Smagorinsky	Smagorinsky	-
Momentum	Bounded central difference (BCD)	Central diff, 2^{nd} order upwind, QUICK	BCD
Pressure	2^{nd} order	Standard	Presto
Energy	QUICK	QUICK	QUICK
Pressure-velocity coupling	Fractional step	SIMPLE	PISO and SIMPLE
Gradient option	Node based	Cell based	Cell based
Transient scheme	NITA	ITA	ITA
Time step	1 ms and 0.25 ms	0.5 ms (and 2 ms)	2 ms and 1ms
No of iterations per time step	-		15 and 30
Density	Curve fit	Boussinesq	Boussinesq and curve fit
Dynamic viscosity	Curve fit	6.58×10^{-7} (const.)	Curve fit
Cp	4178.6 (const.)	4178.6 (const.)	4182.5 (const.)
Thermal Conductivity	0.6306 (const.)	0.6306 (const.)	0.62 (const.)

For details about the models the reader is referred to the Fluent manual. In addition to the LES- and DES-calculations the following computations were also carried out:

- Steady state calculations with the realizable k-ε model for test cases 9 and 10.
- Steady state calculations with standard k-ε, RNG k-ε and differential Reynolds stress model for test case 9.
- Unsteady RANS (URANS) with realizable k-ε (test case 10) and RNG k-ε (test case 11).

Calculations Test 11 (Q_2/Q_1=2.4)

Geometry and mesh

The geometry for the calculations for test 11 is presented in figure 1. Two meshes have been used of approximately 1.3 M and 7.3 M hexahedral cells. The first cell height close to the wall has been chosen to result in Δy+ around 100 for the coarse mesh and 50 for the fine mesh. In the streamwise and circumferential direction (Δx+ and Δs+) the dimensions are around 1500 and 1000 for the coarse mesh and 500 for the fine mesh. Unsteady RANS (RNG k-ε model) and DES calculations were performed for both meshes. In the URANS calculations only results from the fine mesh are presented.

Results

Figures 4 and 5 show fluctuations with high velocity and temperature gradients for the DES cases. The resolved scales in the downstream flow represented by these temperature and velocity fluctuations are not observed in the URANS case. These fluctuations have a large influence on the temperature on the walls. The temperatures four diameters downstream the T-junction for position 0º, 90º and 180º for the experiment and the DES cases are compared in figure 6. The temperature measurements are showing asymmetrical mixing in horizontal plane. The hot water is first reaching the right side of the wall, (0º). The normalised temperature on the right side is around 0.4-0.7 when the left side (180º) is close to 0.

For the DES cases, the global behaviour of the temperature fluctuations is quite realistic. In Figure 6 the temperature is higher on the right side for the fine mesh than for the coarse, which is in better agreement with experiments. None of the simulations reproduces the low temperature at 180º. The temperature fluctuations measured at 0º and 180º are in fact not representative of a tilting of the hot water on the right side but are due to the high vorticity observed in figure 4 close to the wall drawing the hot water against the right wall and the cold against the left, se figure 5 bottom right. The secondary flows caused by the upstream bends affect the mixing process between the hot and cold water. The strength and location of the secondary flow vortices are depending on the mesh and turbulence models as shown by the axial vorticity two diameters upstream in figure 4. A finer mesh results in more concentred vortices that play a larger role on the mixing process. The branch pipe secondary flows show the same dependency on the mesh.

The hot water in the experiment is also reaching the top of the main pipe after only one to two diameters downstream the T-junction [4]. The hot water in the simulations is not coming up as fast to the top of the pipe, but for the fine mesh temperature fluctuations at the top of the pipe three diameters downstream the T-junction were observed.

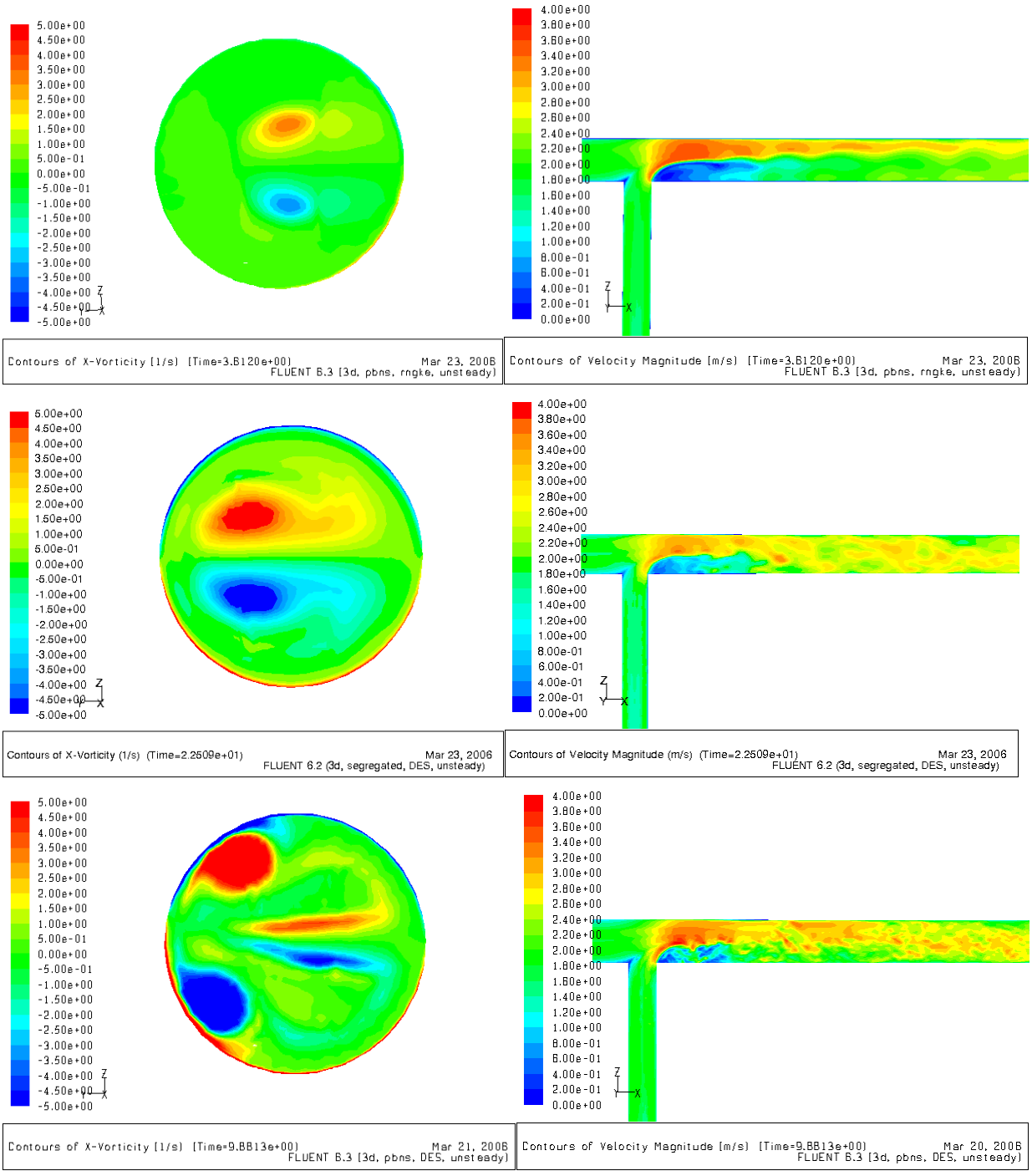

Figure 4 *X vorticity contours in the main pipe 2D upstream the T-junction and instantaneous velocity contours in a vertical plane: Top: URANS, fine mesh; Middle: DES, coarse mesh; Bottom: DES, fine mesh.*

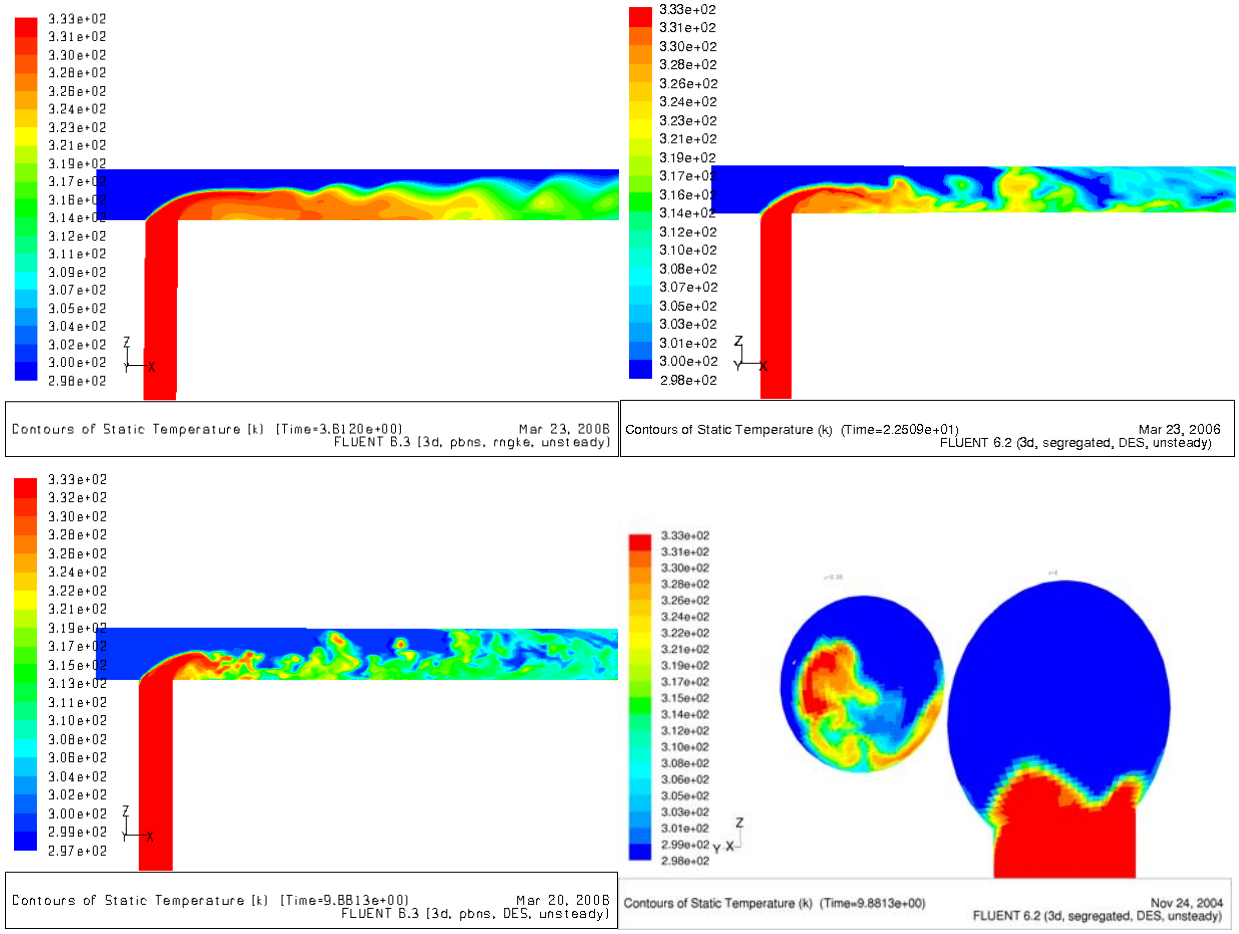

Figure 5 *Temperature contours in a vertical plane: Top left: URANS, fine mesh; Top right: DES, coarse mesh; Bottom left: DES, fine mesh; Bottom right: DES, fine mesh , temperature contours in two axial planes, at the T-junction and two diameters downstream:*

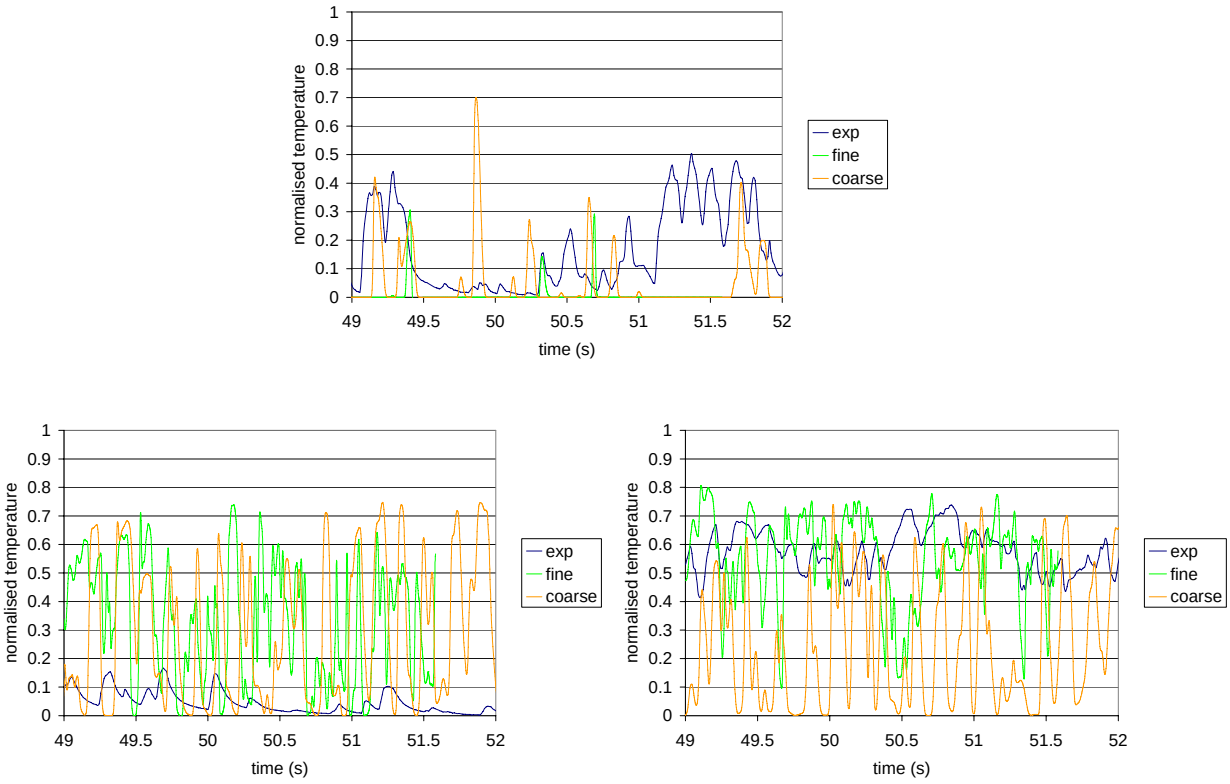

Figure 6 Typical temperature variations at 0º (right), 90º (top) and 180º (left) four diameters downstream the T-junction for the experiment, the DES fine and the coarse meshes.

Calculations Test 10 (Q_2/Q_1=2.8)

For test case 10 both steady and unsteady RANS-calculations as well as Large Eddy Simulations were carried out. Since the test case represents an intermediate flow ratio between test cases 9 and 11, and since most of the results are similar to the ones obtained for the other two cases, no plots are shown here.

It was clear that the steady state calculations predicted a very slow mixing as compared to the experimental results. The unsteady RANS calculations that were carried out gave similar results as the steady state calculations, since the initial fluctuations died out very quickly. However, the different LES-calculations showed considerably better agreement with experiments, although they slightly underpredicted the mixing.

Calculations Test 9 (Q_2/Q_1=5.6)

Geometry and mesh

The calculations were carried out with the same geometry as for Test 10, i.e. the inlet boundaries were located approximately two diameters upstream of the T-junction and the outlet boundary was located ten diameters downstream as shown in Figure 2. A relatively coarse mesh (0.39M cells) was used when testing different inlet boundary conditions and when comparing DES and LES. LES with a finer mesh (1.9M cells) was also carried out to test the grid dependence.

Numerical model and inlet boundary conditions

The unsteady calculations carried out for test case 9 were either based on DES with the Spalart-Allmaras model, or LES with the dynamic Smagorinsky model. In order to account for the upstream bends a steady RANS-calculation was carried out using the numerical model from Onsala Ingenjörsbyrå (see Test 11 above as well as Figure 1), but with flow rates corresponding to Test 9. Mean and turbulence profiles at positions 2D upstream of the T-junction were extracted and used as inlet boundary conditions for the unsteady calculations. To trigger the turbulent fluctuations in the LES different boundary conditions available in Fluent were tested: the spectral synthesizer, the vortex method, as well as a comparison with a calculation using no perturbations at all at the boundaries.

Results

Figure 7 compares instantaneous velocity and temperature fields for DES (coarse mesh), LES (coarse mesh) and LES (fine mesh). It is clear that all calculations exhibit large-scale oscillations downstream of the T-junction, although the flow field predicted with LES contains more small-scale structures than the DES results on the same grid. This observation is more evident when an animation of a time sequence of the flow is studied. A comparison of the turbulent viscosity in the DES with the subgrid turbulent viscosity in the LES showed that the former was considerably larger, which can explain the more damped oscillations in the DES. The temperature fluctuations downstream of the T-junction are violent, and especially in the LES case one can observe hot-water regions also close to the upper wall (Figure 7, right). This is caused by circumferential oscillations that tend to move hot fluid along the pipe wall from the bottom to the upper part of the pipe.

To compare the calculations with available temperature measurements, non-dimensional mean and fluctuating temperatures near the pipe wall are shown in Figure 8. Again the DES-results are compared with corresponding LES, but also results from a LES-calculation using no perturbations at the inlet boundaries are shown. The DES provides a less violent mixing, leading to a slower change in the mean temperature and smaller rms-values than for the corresponding LES. There is an influence of the inlet boundary conditions on the results with LES, but the effect is not dramatic when no inlet perturbations are used. It can also be seen that there is only a moderate change in the results when the mesh resolution is refined.

For test case 9 the best performance was obtained with the LES on the fine mesh, and especially the non-dimensional mean temperatures are in good agreement with available experimental data. Considering the temperature fluctuations the agreement is not as good, and the LES calculation overpredicts the fluctuation level near the bottom wall and the left wall. However, the maximum fluctuation level, which is measured near the right wall (x=380, φ=0°), is close to the simulation result.

Near this maximum the large-scale (low-frequency) part of the calculated spectrum shows fair agreement with the experimental data, but the simulations with the refined mesh contains more energy at higher frequencies (30-100 Hz) than observed in the experiments. Further downstream the decay of the fluctuations is stronger in the experiments than in the calculations, and all LES -cases overpredict the fluctuation level.

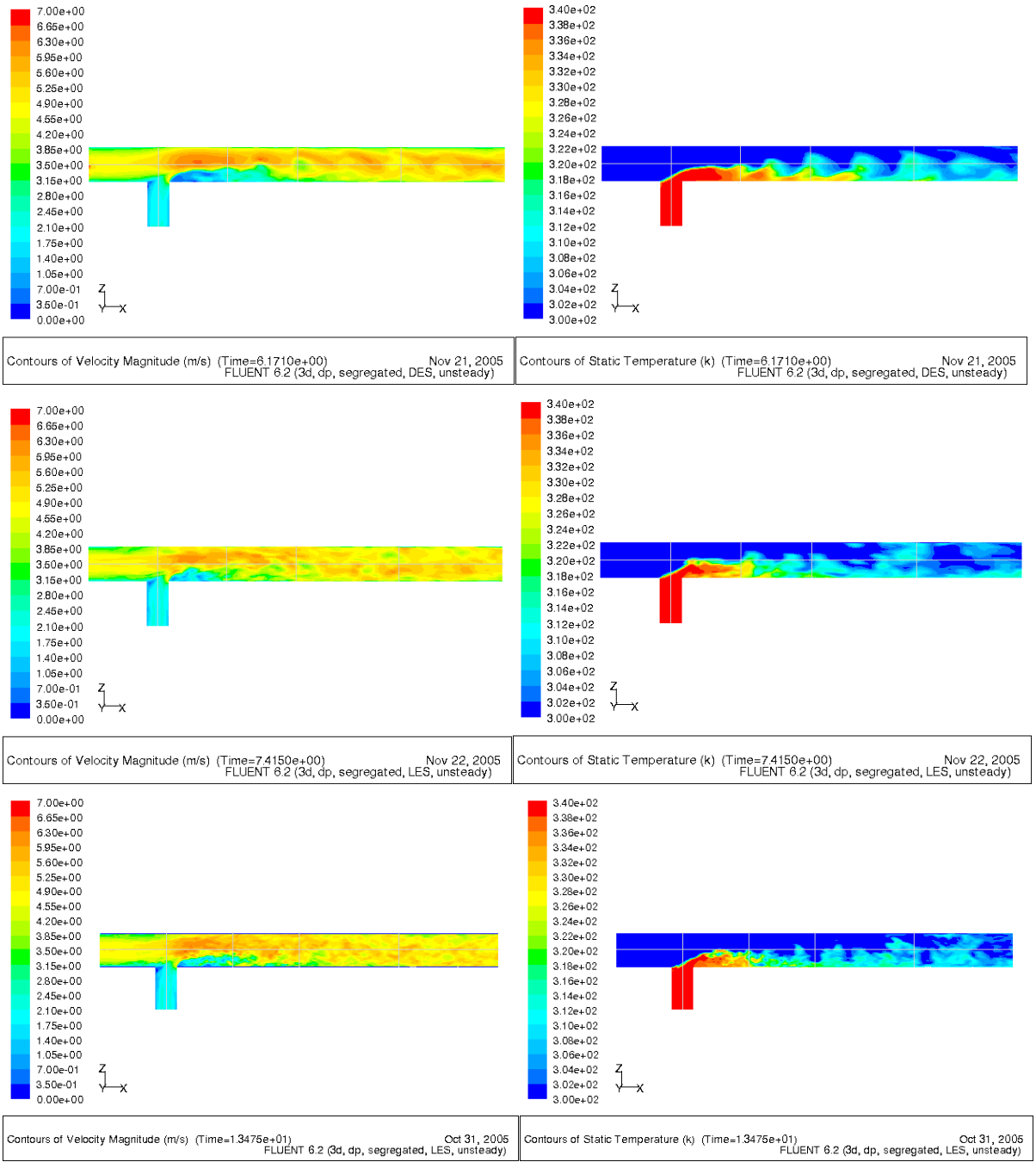

Figure 7 Instantaneous velocity contours (left column) and temperature contours (right column): Top: DES, coarse mesh; Middle: LES, coarse mesh; Bottom: LES, fine mesh.

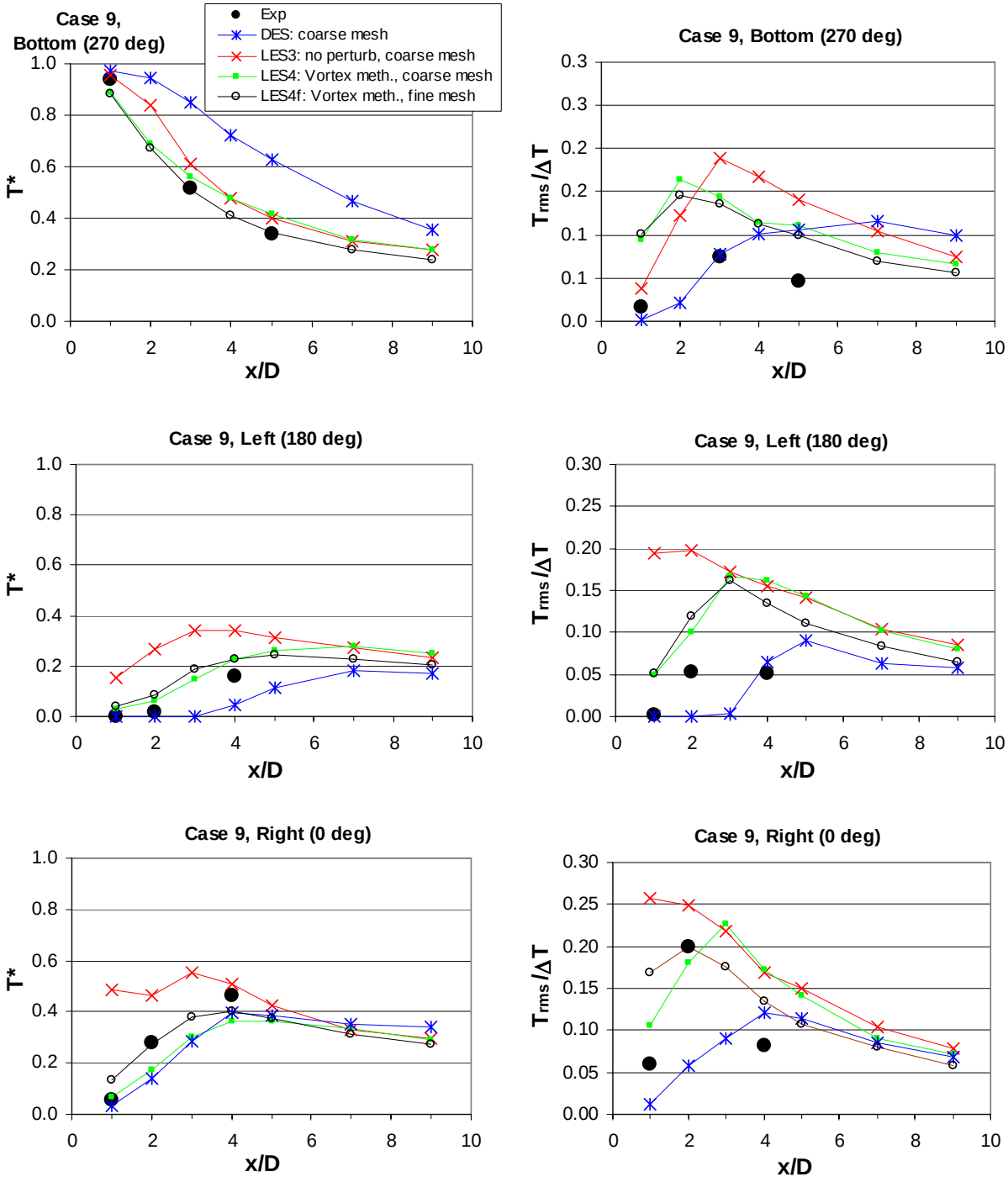

Figure 8 *Non-dimensional mean temperature T* (left column) and temperature fluctuations (right column) for various simulations of test case 9.*

An important question is whether the mesh resolution is fine enough in order to obtain accurate solutions. Since grid independence can usually not be achieved by successive grid refinements, one must rely on other means to estimate whether the resolution is sufficient. For Large Eddy Simulations of wall-bounded flows the recommended mesh resolution results in very large grids. In the present calculations we could not afford such fine mesh resolution, and the law-of-the-wall was applied in the

wall-normal direction together with $(\Delta y^+)_{min}\approx$30-60. In the streamwise and circumferential direction (Δx^+,Δs^+) the cell dimensions were large with about $\Delta x^+\approx$2000 and $\Delta s^+\approx$900 for the coarse mesh and 1000 and 600 for the fine mesh. In the central part of the pipes Δy^+ (and Δz^+) was of the order of 500 and 300 for the two meshes respectively.

Regarding the near-wall flow these cell dimensions are too large for accurate predictions, and it was also observed that it was difficult to sustain turbulent flow in the inlet pipes. However, the calculations nevertheless appear to produce qualitatively realistic results regarding the thermal mixing. Also the grid refinements that were carried out indicated that the key physics for the present case seems to be captured even with the coarse mesh. A plausible assumption is that the characteristic length scale that governs the present flow is not the viscous length scales, but rather length scales associated with the shear layers in the T-junction.

An attempt to estimate integral scales and Taylor micro scales has been undertaken for the present LES calculation, although the estimation is associated with significant uncertainties. The Taylor micro scale (t_0) was estimated from the autocorrelation (R_{uu}) for different separation in time (τ) using a Taylor series expansion:

$$\frac{\tau^2}{1-R_{uu}(\tau)} = t_0^2\left(1+C\tau^2+...\right)$$

Thus, by plotting $\tau^2/(1-R_{uu})$ versus τ^2 and making a linear curvefit to the data, t_0 can be estimated. The integral scale was obtained by integration of the autocorrelation function. The corresponding length scales were then obtained based on Taylor's hypothesis using the mean bulk velocity in the pipe. The estimates were carried out for the LES-calculations with the coarse and a fine mesh, and the spectra for the evaluated signals are shown in Figure 9. The spectra are compared with the standard relation $f^{-5/3}$.

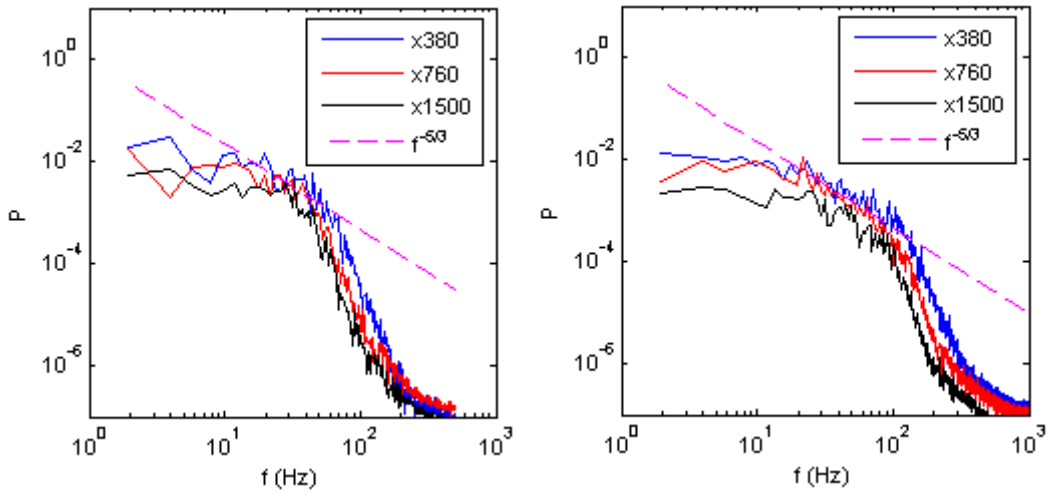

Figure 9 Calculated spectra of the fluctuating velocity of the streamwise component on the centreline at positions x=380 (2D), 760 (4D) and 1500 (7.9D). Left: coarse mesh; Right: fine mesh. Also shown is the line $P=f^{-5/3}$

For the coarse mesh it is hard to find a frequency range with a $f^{-5/3}$-dependence. It was also difficult to find a clear difference in the size of the integral length scales and the Taylor micro scales, with length scales of about 40-55 mm. Considering the streamwise grid spacing (Δx) of about 14 mm in the coarse mesh, and assuming that 2-3 cells are required to resolve a turbulent scale, the minimum

resolvable scale is close to the estimated length scales in the calculated flow field. It is plausible to assume that the detected Taylor micro scales are limited by the mesh resolution and thus not physically correct.

With the refined mesh there is a tendency towards a region with a $f^{-5/3}$-dependence, and the estimated integral and micro scales were also slightly separated in size. The predicted micro time scales are approximately 5 ms, and the corresponding length scales are 25-30 mm. Δx is 6.5 mm in the fine mesh, i.e. the micro scales are about 4 times larger than the mesh spacing. The discussion above should not be considered as a proof that the mesh resolution is sufficient with the finer mesh, rather it is an attempt to relate the mesh spacing to different length scales in order to evaluate the quality of the calculations.

Conclusions

None of the transient calculations described in the present paper can be considered as true LES since the mesh resolution is too coarse near the walls, and consequently the law-of-the-wall has been used. However, despite the fact that the used grids were very coarse for LES the results are quite promising, and it is conjectured that the present flow case, which is dominated by large-scale fluctuations, is well-suited for analysis with LES or DES. Some of the main observations and conclusions are summarized in the following:

- All steady state calculations failed to predict a correct mean temperature near the pipe walls, and common for all tested models is that they severely underpredicted the mixing.
- Calculations using unsteady RANS failed to predict realistic mixing between the two fluids.
- The influence of the upstream boundary conditions is essential on the mixing for case 11 and the main difference due to the mesh sizes is the simulation of the secondary vortices after the upstream bends.
- A comparison between DES and LES on a coarse mesh showed that the fluctuations were more damped for DES when test case 9 was considered. The modelled turbulent viscosity was considerably larger for DES than for LES in this particular case (test 9 with coarse mesh), which could explain the lack of small-scale fluctuations in the DES-case.
- For test case 9 the best results was obtained with LES on a fine mesh. In particular predictions of the mean temperature was in good agreement with the experimental data.
- Considering near-wall temperature fluctuations there are still clear differences between experiments and predictions, and both the DES- and LES-results overpredict the fluctuation level in some regions. Moreover, the calculated spectra show more energy at higher frequencies than observed in the experimental data.
- The present calculations do not provide grid-independent solutions. The grid refinements that were carried out showed that more small-scale fluctuations appeared when a fine mesh was used. However, the predicted mean and rms temperatures near the pipe wall were only moderately affected by the grid refinement.

References

[1] Péniguel, C., Sakiz, M., Benhamadouche, S., Stephan, J.-M. and Vindeirinho, C. (2003) Presentation of a numerical 3D approach to tackle thermal striping in a PWR nuclear T-junction, PVP/DA007, Proceedings of ASME PVP, July 20-24, 2003, Cleveland, USA.

[2] Ohtsuka, M., Kawamura, T, Fukuda, T., Moriya, S., Shiina, K., Kurosaki, M., Minami, Y. and Madarame, H. (2003) LES analysis of fluid temperature fluctuations in a mixing Tee pipe with the same diameters, ICONE 11-36064, 11th International Conference on Nuclear Engineering, Tokyo, Japan, April 20-23, 2003.

[3] Braillard, O., Jarny, Y. and Balmigere, G. (2005) Thermal load determination in the mixing Tee impacted by a turbulent flow generated by two fluids at large gap of temperature, ICONE13-50361, 13th International Conference on Nuclear Engineering, Beijing, China, May 16-20, 2005.

[4] Jungstedt, J., Andersson, M. and Henriksson, M. (2002) Termisk blandning i T-stycke – Resultatrapport. Report U 02:134, Vattenfall Utveckling AB, 2002.

[5] Janobi, M. (2003) CFD calculation of flow and thermal mixing in a T-junction (steady state calculation), Report U 03:69, Vattenfall Utveckling AB.

[6] Westin, J. (2005) Thermal mixing in a T-junction: Steady and unsteady calculations, Report U 05:118, Vattenfall Utveckling AB.

[7] Harleman, M. (2004) Time dependent computations of turbulent thermal mixing in a T-junction. Report FT-2004-685, Forsmarks Kraftgrupp AB.

[8] Veber, P. and Andersson, L. (2004) CFD calculation of flow and thermal mixing in a T-junction – time dependent calculation. Teknisk not 2004/7 Rev 0. Onsala Ingenjörsbyrå AB.

[9] Veber, P. and Andersson, L. (2004) CFD calculation of flow and thermal mixing in a T-junction – time dependent calculation – Part 2. Teknisk not 2004/21 Rev 0. Onsala Ingenjörsbyrå AB.